



## Do envelope solitons radiate?

D. C. CALVO and T. R. AKYLAS

*Department of Mechanical Engineering, Massachusetts Institute of Technology, Cambridge, MA 02139, U.S.A.*

Received 28 January 1998; accepted in revised form 5 January 1999

**Abstract.** In dispersive wave systems, when leading-order nonlinear and dispersive effects are taken into account, the envelope of a small-amplitude narrow-band wave pulse is known to satisfy the nonlinear Schrödinger (NLS) Equation which, under certain conditions, admits envelope-soliton solutions. These solitons describe locally confined wave groups with envelopes of permanent form and find applications in various physical contexts. Here, the question of whether NLS envelope solitons survive when higher-order effects are taken into account is addressed. Based on a kinematic argument first, it is suggested that oscillatory tails are inevitably emitted, and this claim is further supported by numerical computations by use of a fifth-order Korteweg-deVries equation as a simple example. The radiation of tails is caused by a resonance mechanism that lies beyond all orders of the usual multiple-scale expansion leading to the NLS equation, and a procedure for calculating these tails by use of exponential asymptotics is outlined. Despite having exponentially small amplitude in the asymptotic sense, the radiated tails can be significant when pulses of relatively short duration are considered.

**Key words:** nonlinear waves, solitons, water waves, fiber optics, exponential asymptotics.

### 1. Introduction

The nonlinear Schrödinger (NLS) Equation is the canonical evolution equation of the envelope of a small-amplitude narrow-band wave pulse in dispersive wave systems. Ever since it was first derived over thirty years ago [1], the NLS Equation has been instrumental in understanding various nonlinear wave phenomena and it is now considered fundamental to nonlinear wave motion, on equal footing with the celebrated Korteweg-deVries (KdV) Equation that governs the propagation of weakly nonlinear long waves. Among a number of interesting properties that they possess, it is remarkable that both the KdV and the NLS equations are completely integrable via the inverse scattering transform (see, for example, [2, 3]).

Physical motivation for the original derivation of the NLS Equation and for most of the early work on nonlinear dispersive waves in general was drawn from fluid mechanics, especially surface and internal waves with geophysical applications. (A comprehensive review of this body of work can be found in the monograph by Craik [4].) It turns out, however, that many results first obtained for nonlinear waves in fluid flows are also relevant in other applications. In recent years, for example, a popular and rapidly evolving field of research in view of its technological promise is the propagation of electromagnetic wave pulses in optical fibers, and the NLS equation is of central importance in this setting as well [5].

Under conditions that a uniform periodic wavetrain is unstable to modulations – the so-called Benjamin-Feir instability in the context of deep-water gravity waves [6] – the NLS Equation is known to admit envelope-soliton solutions. These correspond to stable, locally confined wave groups with envelopes of permanent form and play an important part in the long-time evolution of a locally confined initial disturbance. Moreover, as they achieve a perfect balance of dispersion and nonlinearity, it was suggested on theoretical grounds [7]

and later demonstrated experimentally [8] that NLS solitary wave pulses are suitable for transmitting data in optical fibers.

In deriving the NLS Equation for the envelope of a narrow-band small-amplitude wave pulse, only the dominant nonlinear and dispersive effects are included. This approximation is bound to fail eventually, however, when higher-order effects come into play after a number of cycles depending on the steepness and the duration of the pulse. For example, according to laboratory observations of deep-water gravity waves in a tank, an initially symmetric pulse with uniform frequency becomes asymmetric after propagating for some distance along the tank [9], whereas the same pulse would remain symmetric based on the NLS Equation. This discrepancy can be explained theoretically by a more accurate envelope equation than the NLS Equation that includes certain nonlinear modulation terms [10, 11], and the same theoretical approach has also been used to study higher-order effects in optical solitons [5, Chapter 8].

In contrast to these prior studies, here we wish to explore a phenomenon that cannot be discussed within the narrow-band approximation, namely the radiation of tails by NLS solitary wave pulses. As it turns out, these tails comprise wavenumbers that, in general, are not sidebands of the carrier wavenumber, so they cannot be properly described by an evolution equation for the wave envelope.

The first indication that NLS solitons may radiate tails was revealed by a numerical study of a modified NLS Equation with a third-order-derivative dispersive term [12]; this third-order NLS Equation replaces the standard NLS in the vicinity of caustics [13], such as the zero-dispersion wavelength in optical fibers. By use of an NLS soliton as initial condition, radiation manifests itself as small-amplitude periodic waves travelling with the same phase speed as the solitary-wave main core. Consequently, NLS envelope solitons become nonlocal – they develop oscillatory tails of non-vanishing amplitude – near caustics [14, 15], and solitary waves of the KdV type also turn out to be nonlocal in certain instances owing to a similar resonance mechanism [16, 17].

In general, however, when the carrier wavelength of a solitary wave pulse is not close to a caustic, the tails implied by the third-order NLS Equation have comparable wavelength to the carrier, violating the slowly-varying-envelope approximation. Therefore, the distinction between the carrier and its envelope is blurred at the tails of the pulse and one has to use the full governing equation rather than an envelope equation to investigate the form of the disturbance there. For this purpose, we shall work with the fifth-order KdV Equation as a simple example of a dispersive wave system that supports solitary pulses of the NLS type.

On the basis of a purely kinematic argument, it is deduced that the wavenumbers that partake in the tails satisfy certain resonance conditions that depend on the dispersion relation of the problem at hand. Hence, given the carrier wavenumber, these resonant wavenumbers can be readily determined, suggesting that solitary pulses radiate tails in general. The tail amplitude cannot be found so easily, however, as it turns out to be exponentially small with respect to the steepness of the main pulse. To calculate the tail amplitude asymptotically, it is necessary to carry beyond all orders the usual multi-scale expansion underlying the NLS Equation, and details are worked out here for solitary pulses governed by the fifth-order KdV Equation.

Despite the fact that the tail amplitude is exponentially small in the asymptotic sense, numerical simulations of the long-time evolution of solitary pulses of the fifth-order KdV Equation indicate that the radiated tails often form a significant part of the overall signal, causing considerable distortion of the main pulse. This suggests that radiation could be an important issue when dealing with solitary pulses of relatively short duration.

## 2. Wave pulses with solitary envelopes

In describing a wave pulse with envelope of permanent form, rather than the space and time variables  $x$  and  $t$ , we find it convenient to use the two phases

$$\theta = k_0(x - ct), \quad \xi = \varepsilon(x - Ct), \quad (1)$$

which move with the carrier and its envelope, respectively,  $c$  and  $C$  being their corresponding speeds. Also, to bring out the fact that the envelope is varying slowly relative to the carrier,  $\xi$  has been scaled with  $0 < \varepsilon \ll 1$ , the ratio of the carrier wavelength  $2\pi/k_0$  to a characteristic lengthscale of the envelope.

In terms of  $\theta$  and  $\xi$ , then, a solitary wave pulse

$$u(x, t) = U(\theta, \xi; \varepsilon) \quad (2)$$

is such that  $U$  is  $2\pi$ -periodic in  $\theta$  and locally confined in  $\xi$

$$U \rightarrow 0, \quad (|\xi| \rightarrow \infty). \quad (3)$$

Generally, the wave profile  $U$  satisfies a nonlinear partial differential equation and is analytically intractable. In the small-amplitude limit, on the other hand, the standard solution procedure is to expand  $U$

$$U = \varepsilon\{A(\xi) e^{i\theta} + \text{c.c.}\} + \varepsilon^2 A_0(\xi) + \varepsilon^2\{A_2(\xi) e^{2i\theta} + \text{c.c.}\} + \dots, \quad (4)$$

as well as

$$c = c_0 + \varepsilon^2 c_2 + \dots, \quad (5a)$$

$$C = c_g|_0 + \varepsilon^2 C_2 + \dots, \quad (5b)$$

here, consistent with the linear theory;  $c_0 = \omega_0/k_0$  denotes the linear phase speed at the carrier wavenumber  $k_0$  and  $c_g|_0 = d\omega/dk|_0$  the corresponding group speed as obtained from the linear dispersion relation  $\omega = \omega(k)$ .

Upon substitution of these expansions in the equation governing  $U$ , the fact that the higher harmonics in the Fourier series (4) are of progressively smaller amplitude allows one to solve for  $A_0, A_2, \dots$  in terms of  $A$ , the envelope of the primary harmonic which turns out to satisfy an evolution equation of the NLS type. Solitary wave pulses, consistent with the condition (3) that they remain locally confined, then correspond to solutions of this evolution equation such that

$$A \rightarrow 0, \quad (|\xi| \rightarrow \infty). \quad (6)$$

Although it is straightforward, the perturbation procedure outlined above typically involves a considerable amount of algebra. In the interest of brevity, here we shall work with a relatively simple example of a dispersive wave system, namely the fifth-order KdV Equation in the normalized form

$$u_t + 6uu_x + u_{xxx} + u_{xxxxx} = 0. \quad (7)$$

In this case, the linear dispersion relation is

$$\omega(k) = -k^3 + k^5 \quad (8)$$

and the details of deriving the evolution equation governing  $A$  have already been worked out in [18]. Specifically

$$A_0 = 6 \frac{|A|^2}{c_g|_0} + O(\varepsilon^2), \quad (9a)$$

$$A_2 = \frac{A^2}{k_0^2(1-5k_0^2)} + 2i\varepsilon \frac{1-10k_0^2}{k_0^3(1-5k_0^2)^2} AA_\xi + O(\varepsilon^2) \quad (9b)$$

and  $A$  satisfies the equation

$$\begin{aligned} & -k_0 c_2 A + \mu A^2 A^* + \lambda A_{\xi\xi} \\ & + i\varepsilon \left[ \gamma A_{\xi\xi\xi} + C_2 A_\xi - \frac{\mu}{k_0} (A^2 A^*)_\xi + \nu |A|^2 A_\xi \right] = O(\varepsilon^2), \end{aligned} \quad (10)$$

where

$$\mu = \frac{6}{k_0} \frac{3-25k_0^2}{(1-5k_0^2)(5k_0^2-3)}, \quad \lambda = k_0(3-10k_0^2),$$

$$\gamma = 10k_0^2 - 1, \quad \nu = \frac{12}{k_0} \frac{1-10k_0^2}{(1-5k_0^2)^2}.$$

In looking for solitary-wave solutions, we find it convenient to introduce the polar form

$$A = S(\xi) e^{i\phi(\xi)}. \quad (11)$$

Upon substitution in (10), it is found that  $S$  and  $\phi$  satisfy

$$\lambda S'' - k_0 c_2 S + \mu S^3 = O(\varepsilon^2), \quad (12a)$$

$$\phi' = -\frac{\varepsilon}{\lambda} \left\{ \gamma \left[ \frac{S''}{S} - \frac{1}{2} \left( \frac{S'}{S} \right)^2 \right] + \frac{1}{2} C_2 + \frac{1}{4} \left( \nu - \frac{3\mu}{k_0} \right) S^2 \right\} + O(\varepsilon^2). \quad (12b)$$

Hence, locally confined solutions for  $S$  consistent with (6) can be obtained only when  $\lambda\mu > 0$  which occurs in the ranges  $\sqrt{3/25} < k_0 < \sqrt{1/5}$  and  $\sqrt{3/10} < k_0 < \sqrt{3/5}$ . Taking  $k_0$  so that this condition is met and normalizing the peak amplitude of the primary harmonic in (4) to be equal to  $\varepsilon$ , we derive the appropriate solution of (12a) as follows

$$S = \frac{1}{2} \operatorname{sech} \beta\xi + O(\varepsilon^2), \quad (13)$$

where

$$\beta = \frac{1}{2} \left( \frac{\mu}{2\lambda} \right)^{1/2}, \quad c_2 = \frac{\mu}{8k_0}.$$

Having determined  $S$ , we can find the phase  $\phi(\xi)$  from (12b). Before doing so, however, to avoid secular terms in expansion (4), we fix the carrier wavenumber to be equal to  $k_0$  at the tails of the pulse:

$$\phi' \rightarrow 0, \quad (|\xi| \rightarrow \infty),$$

making use of (13) and (12b), this condition then specifies  $C_2$

$$C_2 = -\frac{\gamma\mu}{8\lambda}$$

and  $\phi(\xi)$  is given by

$$\phi = \phi_0 + \varepsilon \frac{\sigma}{\beta\lambda} \tanh \beta\xi + O(\varepsilon^2), \quad (14)$$

$\phi_0$  being an arbitrary phase constant and

$$\sigma = \frac{3}{2} \gamma\beta^2 - \frac{1}{16} \left( v - \frac{3\mu}{k_0} \right).$$

Finally, combining (4), (9), (11), (13) and (14), we obtain the following expression, correct to  $O(\varepsilon^2)$ , for a solitary wave pulse

$$U = \varepsilon \operatorname{sech} \beta\xi \cos(\theta + \phi_0) + \varepsilon^2 \left\{ -\frac{\sigma}{\beta\lambda} \operatorname{sech} \beta\xi \tanh \beta\xi \sin(\theta + \phi_0) \right. \\ \left. + \operatorname{sech}^2 \beta\xi \left[ \frac{3}{2c_{g|0}} + \frac{\cos(2\theta + 2\phi_0)}{2k_0^2(1 - 5k_0^2)} \right] \right\} + \dots \quad (15)$$

While the expansion procedure outlined above can be carried to higher order with no apparent difficulty, previous experience indicates that it may still not be justified to conclude that the fifth-order KdV Equation admits solutions in the form of locally confined solitary pulses: solitary waves that are seemingly locally confined based on approximate theories may in fact feature tails that do not decay at infinity [17, 19]; the amplitudes of these tails happen to be exponentially small with respect to that of the main solitary-wave core and cannot be captured by standard perturbation expansions in powers of  $\varepsilon$ , like the expansion (4) used here.

Of course, for such tails to appear, it is necessary that they are kinematically compatible with the main solitary-wave core. In the case of nonlocal solitary waves of the KdV type, for example, the tail wavenumber is such that the corresponding phase speed matches the speed of the main disturbance. But in the present situation where the main pulse cannot be made steady – the carrier and its envelope move at different speeds – this resonance condition is not appropriate. Accordingly, before revising our perturbation procedure to account for possible exponentially small terms, we shall derive, based on a kinematic argument, the conditions that determine whether tails can accompany a solitary pulse in the present setting.

### 3. Resonance conditions

For the purpose of understanding the generation of tails intuitively, it is helpful to think of the main solitary pulse as a known forcing disturbance; out of all possible waves that this

disturbance can excite, only those that are forced resonantly and would appear in the steady-state response can form tails.

More specifically, according to expansion (4), a solitary pulse may be written as

$$U = \varepsilon \sum_{n=-\infty}^{\infty} U_n(\xi; \varepsilon) e^{in\theta}, \quad (16)$$

with  $U_{-n} = U_n^*$ . In this Fourier series, all harmonics other than the primary ( $n = 1$ ) have carriers that, in general, do not satisfy the dispersion relation (8)

$$\omega(nk_0) \neq nk_0c, \quad (n \neq 1) \quad (17)$$

and, hence, are not resonant.

To see how resonance may arise, we decompose the envelope of each harmonic into Fourier components by taking its Fourier transform with respect to  $\xi$

$$\widehat{U}_n(K; \varepsilon) = \frac{1}{2\pi} \int_{-\infty}^{\infty} U_n(\xi; \varepsilon) e^{-iK\xi} d\xi,$$

combining then each of these Fourier components with the corresponding carrier in (16) using (1),  $U$  is seen to comprise terms of the form

$$\widehat{U}_n(K; \varepsilon) \exp\{i[(nk_0 + \varepsilon K)x - (nk_0c + \varepsilon KC)t]\}. \quad (18)$$

From this expression, it is now clear that resonance is possible if for some wavenumber(s)  $K = K_*$ , say, the following condition is met

$$\omega_* = \omega(k_*), \quad (19a)$$

where

$$k_* = nk_0 + \varepsilon K_*, \quad \omega_* = nk_0c + \varepsilon K_*C. \quad (19b)$$

For a given carrier wavenumber  $k_0$  and each harmonic  $n$ , condition (19a) provides an equation to determine  $\varepsilon K_*$ ; the wavenumber  $k_*$  and frequency  $\omega_*$  of the tail corresponding to each real solution of this equation are then given by (19b). For  $n = 0$ , in particular, the mean harmonic in (16) is a long-wave disturbance moving with speed  $C$  and (19a, b) imply that the tail wavenumber  $k_*$  is such that the phase speed of the tail matches  $C$ , consistent with the resonance condition that applies to the tails of solitary waves of the KdV type.

The values of the resonant wavenumbers  $k_*$  that partake in the tails of a solitary wave pulse depend on the linear dispersion relation of the particular problem at hand and can be computed numerically as will be discussed in the next section for the fifth-order KdV Equation. From (19), however, it is clear that, in general, the tail wavenumbers are not sidebands of the carrier wavenumber  $k_0$ , so the tails cannot be described by an evolution equation, like (10), for the envelope of the primary harmonic.

Moreover, in view of (17), conditions (19) indicate that generally  $\varepsilon K_* = O(1)$ ; hence, the tail amplitude, being proportional to  $|\widehat{U}_n(K_*; \varepsilon)|$  according to (18), is expected to be exponentially small with respect to  $\varepsilon$  – the Fourier transform of a smooth function decays exponentially as  $|K| \rightarrow \infty$ . This, in fact, suggests a criterion for determining the asymptotically dominant contribution to the tails: out of all  $k_*$  that satisfy the resonance conditions (19),

the one corresponding to the smallest value of  $|K_*|$  gives the tail with the relatively largest amplitude. On the other hand, to obtain a precise asymptotic expression for the tail amplitude as  $\varepsilon \rightarrow 0$  is not a straightforward matter and requires techniques of exponential asymptotics (see Section 5).

Before proceeding with the asymptotic analysis, we turn to numerical simulations of the evolution of solitary wave pulses of the fifth-order KdV Equation, in an effort to confirm the resonance conditions (19) and to gain further insight into the generation of tails.

#### 4. Numerical evidence

We shall solve the fifth-order KdV Equation (7) numerically using as initial condition expansion (15) correct to  $O(\varepsilon^2)$  which includes only the fundamental, mean and second harmonics ( $n = 1, 0, 2$ , respectively) in the Fourier-series representation (16) of a solitary wave pulse. Thus, attention is focussed on the generation of tails by resonances associated with these three harmonics.

The numerical scheme we used in integrating the fifth-order KdV Equation is the split-step Fourier method [10]. To accommodate radiated waves, the computational domain was expanded, once a threshold value near the boundaries was reached. For most of the computations the step sizes  $\Delta t = 0.0087$ ,  $\Delta x = 0.6$  were used; it was verified that increasing this resolution did not change the results significantly. Also, as a further check, the conservation law

$$\frac{\partial}{\partial t} \int_{-\infty}^{\infty} u^2 dx = 0$$

was satisfied within 0.5%.

As a preliminary step, it is straightforward to find the values of the tail wavenumbers  $k_*^{(n)}$  ( $n = 1, 0, 2$ ) predicted by the resonance conditions (19). Using the dispersion relation (8), we see that they are the real roots of the polynomial

$$k_*^5 - k_*^3 - Ck_* + nk_0(C - c) = 0, \quad (20)$$

where  $c$  and  $C$  are given by (5). Also, based on the resonance mechanism proposed earlier, the wave with the largest amplitude at the tails is induced by the harmonic  $n$  which yields the smallest value of envelope wavenumber  $|K_*^{(n)}|$ . The wavenumber  $k_*^{(n)}$  that, according to this criterion, makes the dominant contribution to the tails is plotted in Figure 1 as a function of the carrier wavenumber  $k_0$  (by use of the lowest-order approximations  $c \approx c_0$ ,  $C \approx c_g|_0$ ).

In interpreting the results of the numerical simulations against the quasi-steady state envisaged in deriving the resonance conditions (19), we observe that the group speed, being the energy-transport speed, plays an important part. Specifically, the front associated with each resonant wavenumber  $k_*^{(n)}$  is expected to propagate with speed  $c_g(k_*^{(n)}) - C$  relative to the main pulse. As a result, it is possible for a resonant wavenumber having a relatively large value of  $|c_g(k_*^{(n)}) - C|$  to generate a tail faster, and be more apparent during the early stages of the pulse evolution, than the asymptotically dominant wavenumber which ultimately contributes the tail with the largest amplitude. Also, since the main pulse has finite energy, the radiation

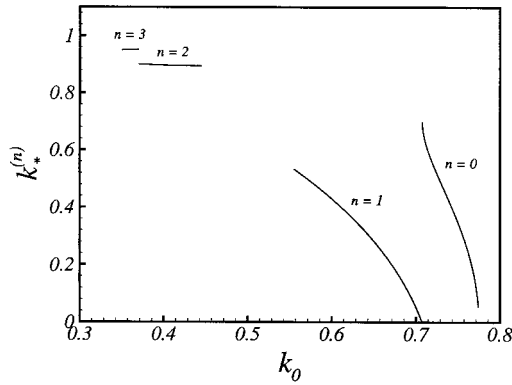


Figure 1. Dominant resonant wavenumbers  $k_*^{(n)}$  plotted as a function of carrier wavenumber  $k_0$  over the two intervals  $\sqrt{3/25} < k_0 < \sqrt{1/5}$  and  $\sqrt{3/10} < k_0 < \sqrt{3/5}$  where the NLS Equation associated with the fifth-order KdV Equation accepts locally confined envelope soliton solutions.

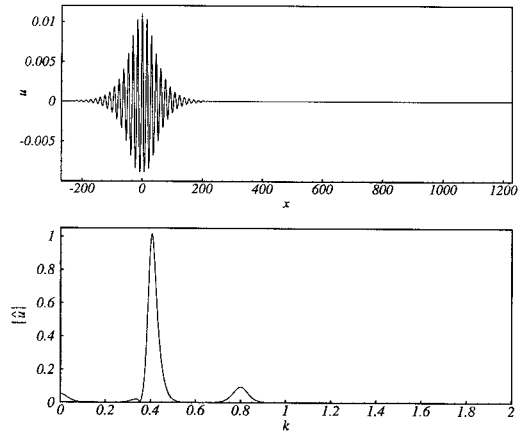
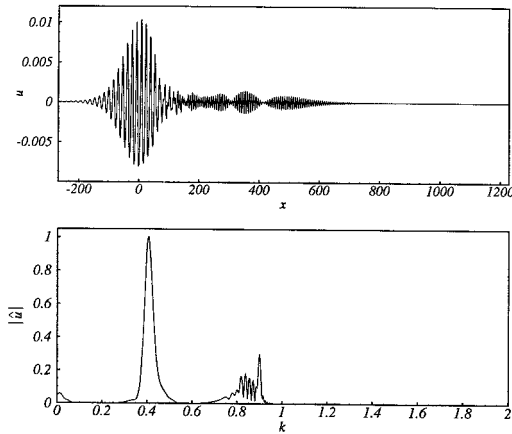
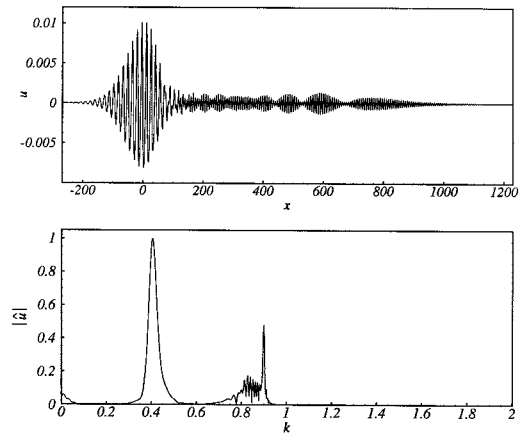


Figure 2a.



(b)



(c)

Figure 2. Pulse evolution shown at the instants (a)  $t = 0$ , (b)  $t = 500$  and (c)  $t = 750$ . Expression (15) is used as the initial condition with parameters  $k_0 = 0.4$ ,  $\varepsilon = 0.01$  and  $\phi_0 = 0$ . The pulse is displayed in both physical (top portion) and wavenumber (bottom portion) spaces. The origin of  $x$  has been chosen to coincide with the pulse center. The magnitude of the spectral amplitude  $|\hat{u}|$  is computed by a base-2 FFT routine using  $N = 4096$  points.

of tails will eventually lead to some loss of form of the wavepacket envelope, this effect being more pronounced as the wave steepness  $\varepsilon$  is increased.

We begin by considering the evolution of a pulse with carrier wavenumber  $k_0 = 0.4$  and steepness  $\varepsilon = 0.01$ . In this instance, the dominant resonant wavenumber according to the



theory is provided by the second harmonic  $n = 2$  (see Figure 1) and, from (19),  $k_*^{(2)} = 0.8971$ . Also since  $c_g(k_*^{(2)}) = 0.82 > 0$  and  $c_g(k_0) = -0.35 < 0$ , one expects radiation to be emitted towards the positive  $x$ -direction, opposite to the propagation direction of the main pulse. Figure 2 shows snapshots of the pulse at  $t = 0$ ,  $t = 500$  and  $t = 750$  along with the corresponding spectra in the wavenumber domain. The initial profile (Figure 2a) is in the form of a packet with approximately 18 cycles within the envelope and, as expected, its spectrum comprises three peaks associated with the fundamental, mean and second harmonics. At  $t = 500$  (Figure 2b), however, a front has developed ahead of the pulse in physical space and a peak is apparent in wavenumber space at  $k \approx 0.9$ , very close to the theoretically predicted resonant wavenumber  $k_*^{(2)}$ . At the later time instant  $t = 750$  (Figure 2c), this peak is even sharper and its attendant radiation more pronounced, with nearly uniform amplitude away from the front.

As a second example, we discuss a pulse with  $k_0 = 0.6$  and  $\varepsilon = 0.02$ . For this carrier wavenumber, conditions (19) predict that the dominant resonant wavenumber (corresponding to the smallest value of  $|K_*|$ ) is  $k_*^{(1)} = 0.4410$  for  $n = 1$ , while the next dominant one (corresponding to the second smallest value of  $|K_*|$ ) is  $k_*^{(2)} = 0.8939$  for  $n = 2$ . A snapshot of the pulse at  $t = 1100$  and the corresponding spectrum are shown in Figure 3. Although a peak is seen in the wavenumber domain at  $k \approx 0.37$  in rough agreement with  $k_*^{(1)}$ , the most striking feature is the dominance of the peak at  $k \approx 0.88$  which is close to  $k_*^{(2)}$ . Note, however, that  $c_g(k_*^{(1)}) - c_g(k_0) = 0.038$ , while  $c_g(k_*^{(2)}) - c_g(k_0) = 1.23$ . Hence, the  $n = 1$  front is very slow and naturally it takes a long time for the corresponding tail to develop relative to the  $n = 2$  front. Also, as these front speeds are positive, the two radiated tails appear ahead of the main pulse, leading to the complicated pattern seen in Figure 3.

Finally, we wish to explore a case in which the  $n = 0$  harmonic in the initial condition furnishes the dominant resonant wavenumber. For  $n = 0$ , Equation (20) in fact reduces to a biquadratic and real roots corresponding to propagating waves can be found only when  $1/\sqrt{2} < k_0 < \sqrt{3/5}$ . Accordingly, we consider a pulse with carrier wavenumber  $k_0 = 0.75$  and steepness  $\varepsilon = 0.025$ . For this choice, it turns out that  $n = 0$  yields both the dominant resonant wavenumber  $k_{*1}^{(0)} = 0.4347$  and the next dominant one  $k_{*2}^{(0)} = 0.9006$  according to

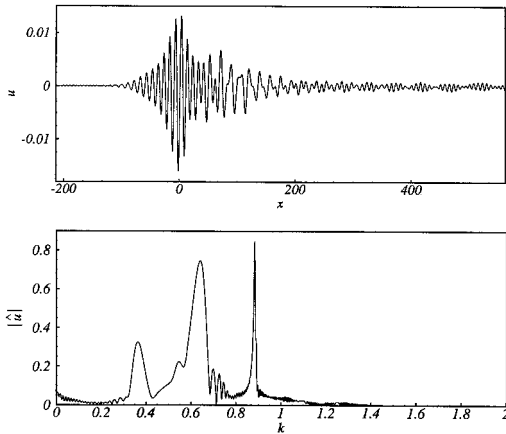


Figure 3. Snapshot of pulse evolution at  $t = 1100$  for the conditions  $k_0 = 0.6$ ,  $\varepsilon = 0.02$  and  $N = 8192$ .

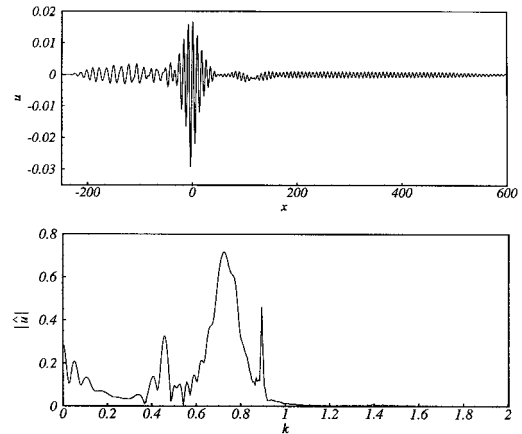


Figure 4. Snapshot of pulse evolution at  $t = 750$  for the conditions  $k_0 = 0.75$ ,  $\varepsilon = 0.025$  and  $N = 2048$ .

the resonance conditions (19). These predictions are confirmed by the results of the numerical simulation at  $t = 750$  shown in Figure 4: there are sharp peaks in the wavenumber domain at  $k \approx 0.44$  and at  $k \approx 0.9$ , in excellent agreement with the theory. Moreover, the radiated tail with the longer wavelength is found behind the main pulse (since  $c_g(k_{*1}^{(0)}) < c_g(k_0)$ ) and has larger amplitude than the other tail which appears ahead of the main pulse (since  $c_g(k_{*2}^{(0)}) > c_g(k_0)$ ).

The numerical results presented thus far certainly support the resonance mechanism proposed earlier; the radiated tails comprise wavenumbers in agreement with those predicted by the resonance conditions (19). More detailed comparisons between analytical and numerical results will be made later, after obtaining an asymptotic expression for the tail amplitude in the weakly nonlinear régime  $\varepsilon \ll 1$ .

## 5. Tail amplitude

On the basis of a heuristic argument, it was deduced in Section 3 that the tails emitted by a small-amplitude solitary wave pulse have exponentially small amplitude with respect to  $\varepsilon$ . This suggests that, in order to capture these tails, it is necessary that we carry expansion (4) beyond all orders in  $\varepsilon$  using techniques of exponential asymptotics.

The procedure for calculating the tail amplitude asymptotically closely parallels that followed in a previous study [20] of steady solitary-wave solutions of the fifth-order KdV Equation in the vicinity of the special carrier wavenumber  $k_0 = 1/\sqrt{2}$  where the phase speed  $c_0$  matches the group speed  $c_g|_0$ . Here, this asymptotic procedure also provides formal justification of the resonance conditions (19) that determine the tail wavenumbers.

The fact that a solitary pulse is accompanied by tails in physical space implies the presence of pole singularities on the real axis at the tail wavenumbers in the wavenumber domain, and the goal is to compute the corresponding residues which determine the tail amplitudes. To this end, it is convenient to work in the wavenumber domain.

We begin by returning to expansion (15) for  $U(\theta, \xi; \varepsilon)$  and taking its Fourier transform with respect to the envelope variable  $\xi$

$$\widehat{U}(\theta, K; \varepsilon) = \varepsilon \operatorname{sech} \frac{\pi K}{2\beta} \left\{ \frac{1}{2\beta} \cos(\theta + \phi_0) + i \frac{\sigma}{2\beta^3 \lambda} \varepsilon K \sin(\theta + \phi_0) + \frac{\varepsilon K}{2\beta^2} \left[ \frac{3}{2c_g|_0} + \frac{\cos(2\theta + 2\phi_0)}{2k_0^2(1 - 5k_0^2)} \right] \coth \frac{\pi K}{2\beta} + \dots \right\}.$$

This expansion becomes non-uniform when  $\varepsilon K = O(1)$  and suggests the uniformly valid two-scale expression

$$\widehat{U} = \varepsilon \operatorname{sech} \frac{\pi K}{2\beta} \widetilde{U}(\theta, \kappa; \varepsilon), \quad (21)$$

where  $\kappa = \varepsilon K$  and

$$\widetilde{U} \sim \frac{1}{2\beta} \cos(\theta + \phi_0) + i \frac{\sigma}{2\beta^3 \lambda} \kappa \sin(\theta + \phi_0) + \frac{|\kappa|}{2\beta^2} \left[ \frac{3}{2c_g|_0} + \frac{\cos(2\theta + 2\phi_0)}{2k_0^2(1 - 5k_0^2)} \right] + \dots, \quad (\kappa \rightarrow 0). \quad (22)$$

Next,  $\tilde{U}(\theta, \kappa; \varepsilon)$ , being  $2\pi$ -periodic in  $\tilde{\theta} = \theta + \phi_0$ , may be expanded in a Fourier series

$$\tilde{U} = \sum_{n=-\infty}^{\infty} \mathcal{A}_n(\kappa; \varepsilon) e^{in\tilde{\theta}}, \quad (23)$$

where, from (22)

$$\mathcal{A}_0 \sim \frac{3}{4\beta^2 c_g|_0} |\kappa| + \dots, \quad (\kappa \rightarrow 0), \quad (24a)$$

$$\mathcal{A}_{\pm 1} \sim \frac{1}{4\beta} \pm \frac{\sigma}{4\beta^3 \lambda} \kappa + \dots, \quad (\kappa \rightarrow 0), \quad (24b)$$

$$\mathcal{A}_{\pm 2} \sim \frac{1}{8\beta^2 k_0^2 (1 - 5k_0^2)} |\kappa| + \dots, \quad (\kappa \rightarrow 0) \quad (24c)$$

and  $\mathcal{A}_n = O(\kappa^{|n|-1})$  for  $|n| > 2$ .

In view of (21) and (23), attention is now focussed on the coefficients  $\mathcal{A}_n$  and their possible singularities on the real  $\kappa$ -axis. Upon substitution of (21) and (23) in the fifth-order KdV Equation (7), after having taken its Fourier transform with respect to  $\xi$ , it follows that the  $\mathcal{A}_n$  are governed by

$$\begin{aligned} & \{\omega(\kappa + nk_0) - C\kappa - nk_0 c\} \mathcal{A}_n \\ & + 3(\kappa + nk_0) \cosh \frac{\pi\kappa}{2\beta\varepsilon} \sum_{p=-\infty}^{\infty} \int_{-\infty}^{\infty} \frac{\mathcal{A}_{n-p}(\kappa - \lambda) \mathcal{A}_p(\lambda)}{\cosh \frac{\pi(\kappa - \lambda)}{2\beta\varepsilon} \cosh \frac{\pi\lambda}{2\beta\varepsilon}} d\lambda = 0, \end{aligned} \quad (25)$$

$$(n = 0, \pm 1, \dots),$$

$\omega(k)$  denoting the linear dispersion relation (8). However, in the limit  $\varepsilon \rightarrow 0$ , the main contribution to the convolution integrals above comes from the ranges  $0 < \lambda < \kappa$  ( $\kappa > 0$ ) and  $\kappa < \lambda < 0$  ( $\kappa < 0$ ). Also, since  $U$  is real,  $\mathcal{A}_{-n}(\kappa) = \mathcal{A}_n(-\kappa)$  on the real  $\kappa$ -axis so it suffices to consider  $\mathcal{A}_n$  ( $n \geq 0$ ) only, and using the leading-order approximations to  $c$  and  $C$  in (5) the equation system (25) is replaced by

$$\begin{aligned} & \{\omega(\kappa + nk_0) - c_g|_0 \kappa - nk_0 c_0\} \mathcal{A}_n + 6(\kappa + nk_0) \sum_{p=0}^n \operatorname{sgn} \kappa \int_0^{\kappa} \mathcal{A}_p(\lambda) \mathcal{A}_{n-p}(\kappa - \lambda) d\lambda \\ & + 12(\kappa + nk_0) \sum_{p=1}^{\infty} \operatorname{sgn} \kappa \int_0^{\kappa} \mathcal{A}_p(-\lambda) \mathcal{A}_{n+p}(\kappa - \lambda) d\lambda = 0, \quad (n \geq 0). \end{aligned} \quad (26)$$

In spite of the fact that it appears more complicated than the original partial differential Equation (7), the integral-equation system (26) is most suitable for analyzing the singularities of  $\mathcal{A}_n(\kappa)$  on the real  $\kappa$ -axis that are of interest here. These singularities are expected to occur at  $\kappa = \kappa_*^{(n)}$ , say, where the coefficient of  $\mathcal{A}_n$  in (26) vanishes. Recalling that  $\kappa = \varepsilon K$ , it is clear to us from (8) and (19) that this happens at the real roots of the polynomial (20) which

in turn correspond to the resonant wavenumbers  $k_*^{(n)} = \kappa_*^{(n)} + nk_0$  (in the limit  $\varepsilon \rightarrow 0$ , so  $c \approx c_0$  and  $C \approx c_g|_0$ ). Hence, the formal asymptotic theory is consistent with the resonance conditions obtained earlier on physical grounds.

The next task is to examine the local behavior of  $\mathcal{A}_n$  close to each singularity at  $\kappa = \kappa_*^{(n)}$  according to the equation system (26). By use of the asymptotic behavior of  $\mathcal{A}_n$  as  $\kappa \rightarrow 0$  noted in (24), dominant balance suggests that

$$\mathcal{A}_n \sim \frac{D_n}{\kappa_*^{(n)} - \kappa}, \quad (\kappa \rightarrow \kappa_*^{(n)}, n > 0), \quad (27a)$$

$$\mathcal{A}_0 \sim \frac{D_0}{\kappa_*^{(0)} \mp \kappa}, \quad (\kappa \rightarrow \pm \kappa_*^{(0)}), \quad (27b)$$

where  $D_n$  ( $n \geq 0$ ) are constants to be determined.

To verify these simple-pole singularities and compute the residues  $D_n$ , we pose the solution to the system (26) in the form of power series as suggested by expansions (24)

$$\mathcal{A}_0 = \sum_{p=2}^{\infty} b_{0,p} |\kappa|^{p-1},$$

$$\mathcal{A}_n = \sum_{p=n}^{\infty} b_{n,p}^{\pm} \kappa^{p-1}, \quad (\kappa \gtrless 0, n > 0),$$

with

$$b_{0,2} = \frac{3}{4\beta^2 c_g|_0}, \quad b_{1,1}^{\pm} = \frac{1}{4\beta}, \quad b_{1,2}^{\pm} = \frac{\sigma}{4\beta^3 \lambda},$$

$$b_{2,2}^+ = -b_{2,2}^- = \frac{1}{8\beta^2 k_0^2 (1 - 5k_0^2)},$$

etc. If we substitute these series in (26), it follows that  $b_{0,2p+1} = 0$ , while the rest of the coefficients satisfy certain recurrence relations that can be readily solved, given the carrier wavenumber  $k_0$ . Based on the asymptotic behavior of  $b_{n,p}$  as  $p \rightarrow \infty$ , one may thus infer the nature of the singularity of  $\mathcal{A}_n$  at  $\kappa = \kappa_*^{(n)}$  and compute the corresponding residue as well. Implementing this procedure, we verified the presence of simple-pole singularities at  $\kappa = \kappa_*^{(2)}$ ,  $\kappa_*^{(1)}$  and  $\kappa_*^{(0)}$ , respectively, for the three choices of  $k_0 = 0.4, 0.6$  and  $0.75$  considered in Section 4, and the results are given in Table 1.

Combining (21) with (23) and (27), each singularity of  $\mathcal{A}_n$  at  $\kappa = \kappa_*^{(n)}$  translates into a singularity of  $\widehat{U}$  at  $K_*^{(n)} = \kappa_*^{(n)}/\varepsilon$ . Moreover, since  $\mathcal{A}_n(\kappa) = \mathcal{A}_{-n}(-\kappa)$  on the real  $\kappa$ -axis, there is an additional simple-pole singularity at  $-K_*^{(n)}$ . Hence

$$\widehat{U} \sim \varepsilon \frac{D_n}{\kappa_*^{(n)} \mp \varepsilon K} \operatorname{sech} \frac{\pi \kappa_*^{(n)}}{2\beta \varepsilon} e^{\pm i n \tilde{\theta}}, \quad (K \rightarrow \pm \kappa_*^{(n)}/\varepsilon, n \geq 0). \quad (28)$$

We note that all these singularities have exponentially small residues and, upon inverting the Fourier transform, the one that contributes the tail with the relatively largest amplitude

Table 1. Numerically determined residues  $D_n$  and parameters appearing in (28) for the dominant  $n = 0, 1$  and 2 resonances.

$k_0$	$n$	$D_n$	$\kappa_*^{(n)}$	$\beta$
0.4	2	0.358	0.0965	2.76
0.6	1	-0.128	-0.170	4.66
0.75	0	-0.369	0.346	4.07

corresponds to the smallest value of  $|\kappa_*^{(n)}|$ , consistent with the heuristic reasoning presented in Section 3.

More specifically, inverting the Fourier transform, we write

$$U = \int_{\mathcal{C}} \widehat{U}(\theta, K; \varepsilon) e^{iK\xi} dK$$

and, since  $\widehat{U}$  has simple poles on the real  $K$ -axis according to (28), the contour  $\mathcal{C}$  is chosen so as to satisfy causality:  $\mathcal{C}$  is indented to pass below (above)  $K = \pm\kappa_*^{(n)}/\varepsilon$  when  $c_g(k_*^{(n)})$  is greater (less) than  $c_g(k_0)$ ,  $k_*^{(n)} = \kappa_*^{(n)} + nk_0$  being the tail wavenumber and  $\omega_*^{(n)} = c_g|_0 \kappa_*^{(n)} + nk_0 c_0$  the corresponding tail frequency. Hence, the induced tail

$$u \sim 8\pi s D_n \exp\left(\frac{-\pi|\kappa_*^{(n)}|}{2\beta\varepsilon}\right) \sin(k_*^{(n)}x - \omega_*^{(n)}t + n\phi_0) \quad (29)$$

is found in  $\xi > 0$  ( $\xi < 0$ ) when  $s > 0$  ( $s < 0$ ) where  $s \equiv \text{sgn}(c_g(k_*^{(n)}) - c_g(k_0))$ . This criterion for determining the position of the tail relative to the main pulse is in line with the results of the numerical simulations in Section 4.

## 6. Discussion

Using the fifth-order KdV Equation as a simple example, we have presented analytical and numerical evidence that solitary wave pulses of the NLS type are accompanied by oscillatory tails owing to a resonance mechanism: each of the harmonics that make up the main pulse, acting as a forcing disturbance, can induce small-amplitude dispersive wave tails of the form (29) either ahead or behind of the main pulse. While the resonant wavenumbers that appear in the radiated tails are determined by this essentially linear process, the precise values of the tail amplitudes are controlled by a fully nonlinear mechanism in which all harmonics are coupled.

The radiation of tails, of course, eventually leads to a decay of the main pulse, but the asymptotic analysis of Section 5 clearly neglects radiation damping. To estimate the time scale over which this approximation is expected to be valid, we recall from basic linear wave theory that the energy flux through an oscillatory tail of constant amplitude is proportional to the square of the tail amplitude. Given that the main pulse has  $O(\varepsilon)$  energy, conservation then implies that radiation damping becomes important when  $t = O(\varepsilon \exp(\pi|\kappa_*^{(n)}|/\beta\varepsilon))$ , where  $n$  corresponds to the dominant radiated tail. For times less than this exponentially long time scale, the pulse envelope is quasi-steady and the radiated tails extend over a long distance in comparison with the envelope lengthscale  $1/\varepsilon$ , as assumed in the asymptotic theory.

Table 2. Comparison of asymptotically predicted and numerically determined tail amplitudes for the  $n = 2$  and  $n = 0$  resonances.

Resonance	$\varepsilon$	Predicted	Numerical
$n = 2$	0.0050	$1.5 \times 10^{-4}$	$9.0 \times 10^{-5}$
	0.0045	$4.5 \times 10^{-5}$	$3.5 \times 10^{-5}$
	0.0040	$9.8 \times 10^{-6}$	$9.8 \times 10^{-6}$
$n = 0$	0.0140	$6.6 \times 10^{-4}$	$2.0 \times 10^{-4}$
	0.0113	$6.7 \times 10^{-5}$	$4.5 \times 10^{-5}$
	0.0100	$1.4 \times 10^{-5}$	$1.2 \times 10^{-5}$

In the weakly nonlinear régime ( $\varepsilon \ll 1$ ), we may then attempt a comparison of the asymptotic result (29) with the tails radiated by a pulse, initially in the form of an NLS solitary wave group given by expansion (15), as it evolves towards the quasi-steady state that the analysis predicts. For this purpose, the carrier wavenumbers  $k_0 = 0.4$  and  $k_0 = 0.75$  are chosen again so the  $n = 2$  and the  $n = 0$  resonances, respectively, contribute the dominant tails. The numerically determined tail amplitudes are averages over 300 cycles in the  $n = 2$  case and 100 cycles in the  $n = 0$  case; this averaging was done after the tails had formed clearly, specifically at time  $t = 6000 - 7000$  for the  $n = 2$  resonance and  $t = 8000 - 9500$  for the  $n = 0$  resonance. For the relatively small values of  $\varepsilon$  considered here, only one peak corresponding to the dominant radiated wavenumber according to the resonance conditions (19) was visible in the wavenumber spectrum. The comparisons are summarized in Table 2.

As expected, agreement between the asymptotic and numerical results improves as  $\varepsilon$  is decreased. On the other hand, for larger values of  $\varepsilon$ , like those used in the simulations depicted in Figures 2 and 4, the asymptotic expression (29) grossly overpredicts the tail amplitude.

Although radiation damping of the main pulse occurs on an exponentially long (with respect to  $\varepsilon$ ) time scale, it is worth emphasizing that the radiated tails develop on a much shorter time scale: as discussed in Section 4, the spatial extent of a radiation front with wavenumber  $k_*^{(n)}$  is controlled by the relative group speed  $c_g(k_*^{(n)}) - c_g(k_0)$  which is essentially independent of  $\varepsilon$ . We must keep this fact in mind when assessing the usefulness of the NLS approach for modelling the long-time dynamics of weakly nonlinear pulses which, according to the NLS theory, evolve on an  $O(1/\varepsilon^2)$  time scale. For instance, if we consider the example with carrier wavenumber  $k_0 = 0.4$  discussed in Section 4 in which the pulse has moderate steepness ( $\varepsilon = 0.01$ ), we find that  $1/\varepsilon^2 = 10,000$  while it is clear from Figure 2 that after only  $t = 750$  the initial signal has been modified substantially owing to the radiated tails, and this would be completely missed by the NLS equation. On the other hand, for a pulse with a very small steepness the radiation amplitude is entirely negligible and the NLS approach is certainly adequate.

Apart from the fifth-order KdV Equation, the mechanism explored here for the generation of tails is expected to be applicable in general to nonlinear dispersive wave systems that admit NLS envelope solitons to leading order. From the resonance conditions (19) it is relatively straightforward to predict the wavenumbers that will be radiated by a pulse in a given system but there is no simple criterion, besides direct numerical simulation, to decide whether the radiation amplitude will be significant for moderate values of the pulse steepness. A relative

measure, however, may be developed using the current study as a guideline. In particular, it may suffice to determine the form of the exponential factor appearing in (29) which is the dominant controlling factor of the radiation amplitude; this requires carrying the asymptotic analysis as far as (21) and computing the values of  $\kappa_*^{(n)}$  which are easily related to the tail wavenumbers  $k_*^{(n)}$ .

Theoretically, the fact that an initially locally confined solitary wave pulse of the NLS type radiates tails of non-decaying amplitude indicates that nonlinear wave pulses with envelopes of permanent form, as predicted by the NLS Equation, would fail to be locally confined in general owing to exponentially small terms. Evidence of this non-local behavior has also been presented in a study by Bryant [21] who investigated oblique wave groups in deep water numerically without invoking the narrow-band assumption. Starting with periodic wave groups, he approached, in the large envelope length-to-carrier wavelength limit, a wave group close to an NLS envelope soliton but with additional small resonant peaks in the wavenumber spectrum. These resonant components satisfied the dispersion relation for deep water waves and amounted to small-amplitude waves outside of the main group.

Nevertheless, it is now known that there exist special circumstances under which locally confined pulses can be obtained. In the case of the fifth-order KdV Equation for instance, steady locally confined wavepackets in the form of solitary waves are possible near the minimum of the phase speed (at  $k_0 = 1/\sqrt{2}$ ) where the phase speed and the group speed can be made equal, and the same is true near the minimum of the gravity-capillary phase speed in the water-wave problem (see [20] and references given therein).

Finally, it is worth pointing out that the amplitude of radiation, although formally exponentially small, can be quite substantial when dealing with pulses of moderate steepness that contain a few carrier cycles within the envelope so the theory presented here would be most valuable to physical settings in which this situation occurs.

### Acknowledgements

Effort sponsored by the Air Force Office of Scientific Research, Air Force Materials Command, USAF, under Grant Numbers F49620-95-1-0047 and F49620-95-1-0443 and by the National Science Foundation Grant Number DMS-9701967.

### References

1. D. J. Benney and A. C. Newell, The propagation of nonlinear wave envelopes. *J. Math. and Phys.* 46 (1967) 133–139.
2. A. C. Newell, *Solitons in Mathematics and Physics*. Philadelphia: SIAM (1985) 244 pp.
3. M. J. Ablowitz and P. A. Clarkson, *Solitons, Nonlinear Evolution Equations and Inverse Scattering*. London Mathematical Society Lecture Notes, 149, Cambridge: Cambridge University Press (1991) 516 pp.
4. A. D. D. Craik, *Wave Interactions and Fluid Flows*. Cambridge: Cambridge University Press (1985) 322 pp.
5. A. Hasegawa, *Optical Solitons in Fibers*. Berlin: Springer-Verlag (1989) 75 pp.
6. T. B. Benjamin, Instability of periodic wavetrains in nonlinear dispersive systems. *Proc. R. Soc. Lond. A* 299 (1967) 59–75.
7. A. Hasegawa and F. D. Tappert, Transmission of stationary nonlinear optical pulses in dispersive dielectric fibers. I. Anomalous dispersion. *Appl. Phys. Lett.* 23 (1973) 142–144.
8. L. F. Mollenauer, R. H. Stolen and J. P. Gordon, Experimental observation of picosecond pulse narrowing and solitons in optical fibers. *Phys. Rev. Lett.* 45 (1980) 1095–1098.
9. M. Y. Su, Evolution of groups of gravity waves with moderate to high steepness. *Phys. Fluids* 26 (1982) 2167–2174.

10. E. Lo and C. C. Mei, A numerical study of water-wave modulation based on a higher-order nonlinear Schrödinger equation. *J. Fluid Mech.* 150 (1985) 395–416.
11. T. R. Akylas, Higher-order modulation effects on solitary wave envelopes in deep water. *J. Fluid Mech.* 198 (1989) 387–397.
12. P. K. A. Wai, C. R. Menyuk, Y. C. Lee and H. H. Chen, Nonlinear pulse propagation in the neighborhood of the zero-dispersion wavelength of monomode optical fibers. *Optics Letters* 11 (1986) 464–466.
13. T. R. Akylas and T.-J. Kung, On nonlinear wave envelopes of permanent form near a caustic. *J. Fluid Mech.* 214 (1990) 489–502.
14. M. Klauder, E. W. Laedke, K. H. Spatschek and S. K. Turitsyn, Pulse propagation in optical fibers near the zero dispersion point. *Phys. Rev. E* 47 (1993) R3844–R3847.
15. D. C. Calvo and T. R. Akylas, On the formation of bound states by interacting nonlocal solitary waves. *Physica D* 101 (1997) 270–288.
16. Y. Pomeau, A. Ramani and B. Grammaticos, Structural stability of the Korteweg-de Vries solitons under perturbation. *Physica D* 31 (1988) 127–134.
17. T. R. Akylas and R. H. J. Grimshaw, Solitary internal waves with oscillatory tails. *J. Fluid Mech.* 242 (1992) 279–298.
18. R. Grimshaw, B. Malomed and E. Benilov, Solitary waves with damped oscillatory tails: an analysis of the fifth-order Korteweg-de Vries equation. *Physica D* 77 (1994) 473–485.
19. T.-S. Yang and T. R. Akylas, Weakly non-local gravity-capillary solitary waves. *Phys. Fluids* 8 (1996) 1506–1514.
20. T.-S. Yang and T. R. Akylas, On asymmetric gravity-capillary solitary waves. *J. Fluid Mech.* 330 (1996) 215–232.
21. P. J. Bryant, Oblique wave groups in deep water. *J. Fluid Mech.* 146 (1984) 1–20.